



# Precious metal-based Catalytic Membrane Reactors for continuous flow catalytic hydrodechlorination

Raúl B. del Olmo<sup>a,\*</sup>, Maria Torres<sup>a</sup>, Julia Nieto-Sandoval<sup>a,b</sup>, Macarena Munoz<sup>a</sup>, Zahara M. de Pedro<sup>a</sup>, Jose A. Casas<sup>a</sup>

<sup>a</sup> Chemical Engineering Department, Universidad Autónoma de Madrid, Colmenar km 15, Madrid 28049, Spain

<sup>b</sup> Department of Chemical Engineering and Analytical Chemistry, Faculty of Chemistry, Universitat de Barcelona, C/Martí i Franqués 1, Barcelona 08028, Spain

## ARTICLE INFO

### Keywords:

Catalytic hydrodechlorination  
Catalytic Membrane Reactors  
Prochloraz  
Pd  
Rh  
Water treatment

## ABSTRACT

This work is focused on the development of Catalytic Membrane Reactors (CMRs) comprising precious metals as active phases for a comparative assessment in continuous-flow catalytic hydrodechlorination (HDC). HDC has proved its remarkable potential for application as polishing step in drinking water treatment plants, but studies operating in continuous mode are scarce. Preliminary experiments were conducted in batch operation using Pd/Al<sub>2</sub>O<sub>3</sub>, Rh/Al<sub>2</sub>O<sub>3</sub> and Pt/Al<sub>2</sub>O<sub>3</sub> powder catalysts to evaluate the influence of the active phase on the removal of prochloraz (PCZ) (100 µg L<sup>-1</sup>), a pesticide listed on the EU Watch List (2022/1307), by HDC. PCZ removal was successfully described by a pseudo-first order kinetic equation and reaction pathways were proposed. Among the catalysts tested, Pt-based suffered a significant deactivation, not warranting the elimination of this micro-pollutant. Pd/Al<sub>2</sub>O<sub>3</sub> exhibited a faster removal of PCZ than Rh/Al<sub>2</sub>O<sub>3</sub>, while this catalyst resulted in further hydrogenation of the non-chlorinated reaction product. Accordingly, different CMRs were developed by decorating cylindrical inert porous alumina membranes with Pd, Rh, and a combination of Pd-Rh as active phases (~1% wt.). All CMRs showed a remarkable stability along 100 h on stream, being Pd/CMR be the most effective, with a pseudo-first order rate constant value of 0.062 min<sup>-1</sup>. An assessment of the impact of operating conditions (aqueous flow rate, PCZ initial concentration, temperature and H<sub>2</sub> flow rate) was conducted using the Pd/CMR, which notably remained stable for 450 h on stream. The versatility of the system was finally demonstrated in tap water, achieving a steady-state PCZ conversion close to 95 %.

## 1. Introduction

Water pollution resulting from poorly managed wastewater treatments represents a significant threat for both the environment and public health [1]. This issue is aggravated by the occurrence of emerging contaminants, being azole compounds a particularly hazardous micro-pollutant family [2]. Given their harmful character, these chemicals, commonly present in most fungicides and certain drugs [3] were included in the EU Watch List (Decision 1161/2020) of substances for monitoring and risk assessment in EU water basins. Among them, prochloraz (PCZ), an organochlorinated azole compound widely used as a cereal fungicide since 1977 [4], is one of the most commonly detected in aquatic ecosystems. PCZ has been found in fresh surface waters at concentrations on the order of ng L<sup>-1</sup>, such as in the Júcar River (Spain), where detected levels range between 70 and 80 ng L<sup>-1</sup> according to various studies in the literature [5,6]. Apart from its widespread

distribution, PCZ exhibits a remarkable ecotoxicity towards aquatic organisms, with reported LC<sub>50</sub> values of 3.4 mg L<sup>-1</sup> and 6 µg L<sup>-1</sup> for *Artemia salina* and *Gammarus pulex*, respectively [7,8].

Conventional drinking water treatment plants (DWTPs) lack the ability to eliminate micropollutants as they were not selectively designed for such goal. Elfikrie et al. (2020) [9] assessed the removal of several pesticides (tebuconazole, buprofezin, imidacloprid...) from the Tengi River in Colombia via a DWTP, highlighting that conventional processes failed to completely remove these micropollutants. Pesticide removal efficiencies in conventional DWTP were 77 % for imidacloprid, 86 % for buprofezin and 88 % for tebuconazole. Among the various alternatives evaluated by the authors, the adsorption process allowed achieving high removal efficiencies. Similarly, Adams et al. (2002) [10] reported 80 % elimination of azole compounds using activated carbon as adsorbent. While achieving high removal yields, adsorption processes face significant practical limitations, mainly the need for periodic

\* Corresponding author.

E-mail address: [raul.benitod@uam.es](mailto:raul.benitod@uam.es) (R.B. del Olmo).

<https://doi.org/10.1016/j.jece.2024.112754>

Received 24 January 2024; Received in revised form 19 March 2024; Accepted 8 April 2024

Available online 12 April 2024

2213-3437/© 2024 The Author(s). Published by Elsevier Ltd. This is an open access article under the CC BY-NC license (<http://creativecommons.org/licenses/by-nc/4.0/>).

regeneration of the adsorbent upon saturation, leading to additional costs [9].

In this context, catalytic hydrodehalogenation (HDH) emerges as an innovative technology for the elimination of organohalogenated micropollutants, the most harmful ones given their long-term persistence, strong bioaccumulation potential and high toxicity [11,12]. This process involves exposing the organohalogenated pollutant to a hydrogen stream in the presence of a precious metal-based solid catalyst. After the HDH reaction, a halogen-free product is obtained with the formation of the corresponding halogen hydride [13,14]. Pd-based catalysts are commonly employed and have shown high efficiency in removing a wide variety of organohalogenated micropollutants, while alumina is commonly used as catalyst support given its high mechanical strength and its strong interaction with precious metals leading to enhanced metal dispersion [15]. In our previous work, complete removal of a mixture of azole compounds from several aqueous matrices was accomplished via HDH in the presence of a Pd/Al<sub>2</sub>O<sub>3</sub> powder catalyst. Remarkably, a dramatic reduction in the ecotoxicity of these samples was observed in the reaction effluents [16]. According to the literature, the use of other active phases such as Rh, Pt, Ag, Cu, Ni or a combination of them, could promote the hydrogenation of the pollutants and increase reaction rates [17,18]. Wang et al. (2015) [19] synthesized bimetallic Au-Pd nanoparticles for the HDC of DCF (30 mg L<sup>-1</sup>, pH=7, [catalyst]= 56 mg L<sup>-1</sup> and in H<sub>2</sub> atmosphere). Their study demonstrated that the synergistic effect of both metals achieved a remarkable 95% conversion, surpassing the negligible or considerably lower activity observed when each metal was individually used (conversion yields below 20 %). Calvo et al. (2008) [20] assessed the catalytic activity of powdered Pd, Cu, and Ni catalysts supported on activated carbon for the HDC of alachlor (50 mg L<sup>-1</sup>) in aqueous phase employing diluted H<sub>2</sub> in N<sub>2</sub> as the reducing agent. The experiments were conducted in a continuous trickle-bed reactor. Notably, the Pd catalyst exhibited superior activity, achieving alachlor conversion values close to 90 % and a significant ecotoxicity reduction (90 %).

The activity of different precious metals as active phases in powder catalysts has been previously investigated in the literature [21,22], but operating mainly in batch operation. The scale-up of HDC using those catalytic systems poses significant limitations since fixed-bed reactors often leads to significant pressure drops [23,24]. On the other hand, achieving optimal mixing and maintaining ideal flow conditions for H<sub>2</sub> is also critical during the HDC process [25,26]. One promising alternative to address these challenging issues is the use of Catalytic Membrane Reactors (CMRs), which consist of a porous cylindrical membrane decorated with metal nanoparticles on its external surface. The membrane serves as an interface between the aqueous phase circulating on the outside and the gas fed from the inside, which is uniformly distributed throughout the pores toward the outer surface [27]. The reaction occurs at the membrane outer surface favouring the contact between the three phases [28]. Although CMRs have been assessed for other catalytic processes [29,30], there is a lack of studies focused on the HDC of organohalogenated pollutants. Promising results were obtained by Luo et al., (2020) [31] for the dechlorination of 1,1,1-trichloroethane and trichloroethene using Pd nanoparticles deposited on hollow fiber membranes achieving high conversions values (>95 %) upon 90 d of operation. Similarly, in our previous work, a CMR was developed by decorating a porous alumina membrane with Pd nanoparticles. This catalytic system exhibited high activity (80 % conversion values) and stability (over 200 h on stream) in the catalytic hydrodechlorination (HDC) of diclofenac [28].

This work aims to develop active and stable CMRs as catalytic reaction systems for the continuous HDC reaction applied to the treatment of water contaminated with organochlorinated compounds. The development of such continuous reaction systems is essential for the future scaling of the process and its implementation in a water treatment plant. In a preliminary set of experiments, the HDC kinetics was evaluated using a batch-mode slurry reactor, comparing the activity of several

commercial alumina-supported powder catalysts containing different active phases (Pd, Rh and Pt). Based on the obtained results, reaction pathways were proposed for each catalyst considering the intermediates and reaction products identified. Afterwards, monometallic and bimetallic CMRs using Pd and Rh as active phases were developed to assess their performance in the continuous HDC of PCZ. The impact of operating conditions, including the flow rates of both aqueous and H<sub>2</sub> streams, temperature and the initial PCZ concentration on the performance of CMRs was investigated. Furthermore, the stability of the CMRs and the versatility of the most promising reaction system for treating a representative aqueous stream (tap water spiked with PCZ) were evaluated.

## 2. Materials and methods

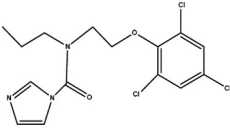
### 2.1. Materials

The structure of PCZ, which was provided by Sigma-Aldrich (≥98%), and its main properties are summarized in Table 1. Palladium (II) chloride salt (anhydrous, 60 %), sodium carbonate (99.8 %) and sodium bicarbonate (99.9 %) were also supplied by Sigma-Aldrich. Hydrochloric acid (37%) was provided by PanReac. Acetonitrile (99.9 %) and hydrogen (99.999 %) were obtained from Fisher Scientific and Praxair, respectively. The commercial catalysts Pd/Al<sub>2</sub>O<sub>3</sub> (Lot: U20A021), Rh/Al<sub>2</sub>O<sub>3</sub> (Lot: U27A030) and Pt/Al<sub>2</sub>O<sub>3</sub> (Lot: M15F051) (1 % wt.) were supplied by Alfa Aesar in powder form. All experiments were carried out using deionized water, unless otherwise indicated.

### 2.2. Catalytic Membrane Reactors preparation

Commercial porous alumina membrane tubes (Auxiaqua) with a pore diameter of 0.8 μm, 12 cm in length, 1 cm external diameter and 4 mm in thickness were used as the starting material for CMRs preparation. The preparation of the catalytic membrane reactors consisted of four stages: ionic adsorption, drying, calcination and reduction. For the incorporation of the active phase (Pd, Rh or Pd-Rh), the alumina membrane was introduced vertically into a 25 mL test tube containing 18 mL of a 50 g L<sup>-1</sup> solution of the metal chloride to be impregnated. The precursors of the active phases were prepared in each case using PdCl<sub>2</sub> or RhCl<sub>3</sub> salts. In the case of the bimetallic catalytic membrane, a 50 wt% solution of each salt was used. The pH of the solution was adjusted to 1 with diluted HCl. The ionic adsorption of the metallic active phase takes place at acidic pH because these conditions favor the deposition of metals on the surface of alumina [32,33]. To ensure that the active phase was deposited only on the outer surface of the membrane, a seal was applied at the bottom of the tube. Additionally, a continuous flow of N<sub>2</sub> gas was introduced from the top of the tube to displace it inside the pores of the membrane, preventing their impregnation and blockage. To achieve an adequate metal loading in the CMRs, successive cycles of 30 min of ionic adsorption were carried out with the membrane being immersed in the metal chloride solution. Between each cycle, a gentle stream of air to the external surface was applied to remove the solution excess and the materials were dried in a microwave oven at 700 W power for 10 min, rotating them periodically every 10 s to achieve a homogeneous drying. Fourteen cycles of ionic adsorption-drying were conducted in all cases. At this point, there was no weight modifications of the membrane compared to the previous cycle, i.e., no additional incorporation of active phase was achieved. Subsequently, the materials underwent oven drying at 60 °C for 24 h. Following the drying step, the CMRs were calcined in air atmosphere using a muffle furnace with a temperature ramp of 2 °C min<sup>-1</sup> from ambient temperature to 300 °C and then maintained for 4 h, with the aim of fixing the active phases on the membrane. The final stage, intended to obtain an appropriate ratio of the zero-valent/electrodeposited species of the active metal in the CMRs, involved reduction in a vertical furnace with an H<sub>2</sub> flow rate of

**Table 1**  
Properties of the prochloraz.

Compound	Abbreviation	Structure	pKa	Molecular weight (g mol <sup>-1</sup> )
Prochloraz	PCZ		3.8 (Stutz and Malissa, 1998)	376.67

100 N mL min<sup>-1</sup>, at a heating rate of 5 °C min<sup>-1</sup>, maintaining a temperature of 150 °C for 2 h [28].

### 2.3. Catalysts characterization

Both the commercial powder catalysts and the developed catalytic membranes were characterized (the latter were characterized by cutting a piece of the cross-section (before and after use)). The textural properties of the CMRs were characterized by nitrogen adsorption-desorption at -196 °C using a Micromeritics Tristar 3020 equipment. The membranes were firstly degassed overnight at 150 °C at a residual pressure of < 10<sup>-3</sup> torr. Pd and Rh contents were determined by inductively coupled plasma mass spectrometry (ICP-MS) using a Perkin Elmer NexION 300 X instrument. An Ar plasma with a temperature of 10,000 K and a radio frequency of 1100 W were used. The metals were subjected to a digestion process in a high-pressure microwave digester using 8 mL HNO<sub>3</sub> + 2 mL H<sub>2</sub>O<sub>2</sub> + 1 mL HF as digestion solution. Elemental analyses of fresh and used catalysts were carried out using a LECO CHNS-932 Elemental Analyzer. Transmission electron microscopy (TEM) images of fresh and used Pd/CMR, Rh/CMR and Pd-Rh/CMR were obtained using a JEOL JEM 2100 microscope. ImageJ software was used to measure palladium and rhodium nanoparticles size from the digital TEM images (more than 200 particles were measured per sample) to obtain the average metal particle diameter. X-ray photoelectric spectroscopy (XPS) was employed to determine the surface content of Pd and Rh on the catalysts using a PHI VersaProbe II spectrometer equipped with an Al K $\alpha$ , 1486.6 eV X-ray excitation source. XPS-Peak software was used for peak deconvolution, and the ratio of Pd<sup>0</sup>/Pd<sup>n+</sup> or Rh<sup>0</sup>/Rh<sup>n+</sup> species on the CMRs surface was calculated from the spectral peak areas obtained for each species.

### 2.4. Experimental procedure

Batch HDC reactions were carried out in a 500 mL glass reactor. In each run, a volume of 450 mL of the PCZ solution with the selected powdered catalyst was introduced into the reactor. Once the solution was heated to the desired temperature using the magneto-heating reactor plate, the reactions were initiated by continuously feeding 50 N mL min<sup>-1</sup> of H<sub>2</sub>. To ensure uniform gas distribution, it was introduced through a diffuser at the bottom of the reactor.

Unless otherwise indicated, experiments were conducted with an initial PCZ concentration of 100  $\mu$ g L<sup>-1</sup> in deionised water. To aid in identifying intermediates, products and to establishing the chlorine balance throughout the reactions, additional tests were carried out using a significantly higher concentration of PCZ (10 mg L<sup>-1</sup>).

The activity of three commercial precious metal-based catalysts supported on alumina (Pd/Al<sub>2</sub>O<sub>3</sub>, Rh/Al<sub>2</sub>O<sub>3</sub> and Pt/Al<sub>2</sub>O<sub>3</sub>), whose concentration in the reaction medium was 0.25 g L<sup>-1</sup>, was evaluated. The reactions were carried out at 25 °C stirring at 900 rpm to avoid external diffusion limitations [34]. The batch HDC study was completed with PCZ adsorption tests on the different catalysts under the same operating conditions, but in the absence of hydrogen. Samples were periodically collected throughout the reaction (or adsorption) tests and analysed immediately. Prior to analysis, the catalyst was separated from the aqueous medium by centrifugation at 10,000 rpm using an Orto Alresa centrifuge (Minicen) for 1 min.

Continuous aqueous-phase HDC reactions using the developed CMRs were conducted in a double-jacketed glass tube reactor, continuously fed with an aqueous stream in an up-flow mode at 25 °C. The membrane was located in the center of the tubular reactor, and a continuous H<sub>2</sub> gas stream was introduced into the membrane core ensuring a flow of this reagent to the active sites on the outer surface. The stability of the membrane was evaluated in a long-term continuous experiment (up to 100 h on stream). The main variables evaluated were aqueous solution flow rate (0.75–2 mL min<sup>-1</sup>), H<sub>2</sub> gas flow rate (5–50 N mL min<sup>-1</sup>), temperature (20–40 °C) and initial PCZ concentration (100–250  $\mu$ g L<sup>-1</sup>). Finally, the versatility of the reaction system was evaluated in using tap water as reaction matrix. In all continuous HDC reactions, liquid samples from the effluent were analysed.

PCZ and its reaction intermediates were quantified by HPLC-UV (Prostar, Varian model 410) using an Eclipse Plus C18 column (15 cm length) at 212 nm. A mixture of acetonitrile and deionised water (60/40 % v/v) was used as mobile phase. The method was operated in isocratic mode and the total chromatographic run time was 10 min. The resulting intermediates and products were identified by LC/MS (Agilent 6120 Single Quadrupole mass spectrometric detector equipped with an electrospray ionization (ESI) source) using the same column and conditions previously described. The intermediates were tentatively identified, corresponding the mass values found with the structure of the proposed intermediates. The LC/MSD ChemStation software package was applied for data acquisition and processing. Chlorides released during PCZ hydrodechlorination were quantified by ion chromatography (Metrohm 883 Basic IC Plus) using an anion exchange column (Metrosep model ASupp 5 250/4.0). The mobile phase consisted of a mixture of Na<sub>2</sub>CO<sub>3</sub>/NaHCO<sub>3</sub> with a concentration of 3.2 mM/1 mM, respectively.

## 3. Results and discussion

### 3.1. HDC of PCZ with Pd/Al<sub>2</sub>O<sub>3</sub>, Rh/Al<sub>2</sub>O<sub>3</sub>, and Pt/Al<sub>2</sub>O<sub>3</sub>, powder catalysts

The main characteristics of the commercial powder catalysts (mean particle size ranging from 45.3 to 47.5  $\mu$ m) used in this work are summarized in Table 2 and described in more detail in our previous work [17]. It should be noted that the metal content in the three catalysts (Pd/Al<sub>2</sub>O<sub>3</sub>, Rh/Al<sub>2</sub>O<sub>3</sub> and Pt/Al<sub>2</sub>O<sub>3</sub>) was close to the nominal 1% wt., and the ratio of metal/electrode deficient species (Me<sup>0</sup>/Me<sup>n+</sup>) on the catalyst surface was approximately 1 in all cases, which is considered the optimum for HDC promoted by precious metal-based catalysts [21]. On the other hand, the size of the metal nanoparticles in the Pd and Pt catalysts was somehow higher than that of Rh, although a high dispersion of the active phase on the catalyst surface was confirmed in all cases. Finally, no significant differences were observed in the surface

**Table 2**  
Characterization of the powder catalysts.

	M (%wt.)	M <sup>0</sup> /M <sup>n+</sup>	dp (nm)	BET (m <sup>2</sup> g <sup>-1</sup> )
Pd/Al <sub>2</sub> O <sub>3</sub>	0.95	1.04	3.3	147
Rh/Al <sub>2</sub> O <sub>3</sub>	0.91	1.13	1.7	153
Pt/Al <sub>2</sub> O <sub>3</sub>	0.85	1.48	3.6	128

area of the three catalysts.

Batch-mode PCZ hydrodechlorination experiments were carried out to assess the activity of different active phases, using Pd/Al<sub>2</sub>O<sub>3</sub>, Rh/Al<sub>2</sub>O<sub>3</sub> and Pt/Al<sub>2</sub>O<sub>3</sub> commercial powder catalysts. Fig. 1 shows the performance of the catalysts in the HDC of PCZ. All catalysts were active for PCZ degradation, but notable variations were observed depending on the active phase employed. The Pd/Al<sub>2</sub>O<sub>3</sub> catalyst emerged as the most effective one, showing a remarkable reaction rate and reaching a PCZ conversion >99 % within 20 min reaction time. The Rh/Al<sub>2</sub>O<sub>3</sub> catalyst also demonstrated a reasonable activity, reaching complete PCZ removal in around 40 min. In contrast, although the Pt/Al<sub>2</sub>O<sub>3</sub> catalyst initially exhibited a degradation rate somewhat higher than the exhibited by the Rh/Al<sub>2</sub>O<sub>3</sub> catalyst, a remarkable decrease in reaction rate was observed after a few minutes of reaction. Over extended reaction times the degradation rate was clearly decreased, ultimately resulting in a PCZ conversion of only 60 % after 1 h reaction time. The evolution in Pt/Al<sub>2</sub>O<sub>3</sub> performance might be attributed to a progressive deactivation of this catalyst, whose active centers seem to be progressively deactivated by the HCl produced during the reaction. This deactivation phenomenon has been reported in a prior study [35], suggesting the susceptibility of Pt/Al<sub>2</sub>O<sub>3</sub> to chloride poisoning effects.

The abovementioned results demonstrated a clear effect of the active phase on the activity exhibited by the catalysts during the hydrodechlorination of PCZ. Whereas Pd/Al<sub>2</sub>O<sub>3</sub> and Rh/Al<sub>2</sub>O<sub>3</sub> catalysts showed fast and efficient PCZ removal making them suitable for high-performance HDC applications, Pt/Al<sub>2</sub>O<sub>3</sub> catalyst, while initially competitive, exhibited significant deactivation over time, highlighting the need for further investigations into catalyst regeneration strategies.

The evolution of PCZ concentration along HDC with the different catalysts can be described according to a pseudo-first-order kinetic equation. HDC kinetic rate constants for each catalyst were accordingly obtained with high correlation coefficients (see Fig S1 of Supplementary Material for experimental data fitting). As can be seen in Table 3, the reaction rate followed the order: Pd/Al<sub>2</sub>O<sub>3</sub> > Rh/Al<sub>2</sub>O<sub>3</sub> > Pt/Al<sub>2</sub>O<sub>3</sub>. Similar results were reported by Dini et al., 1975 [36] when evaluating the catalytic activity of Pt, Rh and Pd-poly-p-p-phenylene terephthalamide catalysts in the context of chlorobenzene hydrodechlorination. Their study revealed a consistent trend of decreasing chlorobenzene conversion, in accordance with the sequence Pd > Rh > Pt, which aligns with the findings in our study. The higher activity exhibited by the Pd catalyst seems to be related both to the appropriate size of Pd particles acting as the catalytic active phase and the resistance of this metal to poisoning by HCl. In fact, Díaz et al. (2011) [22] in their study on the HDC of chlorophenols established a metal particle size between 3 and 4 nm as optimal for precious metals constituting the active phases of HDC catalysts. Rhodium showed a lower dechlorination

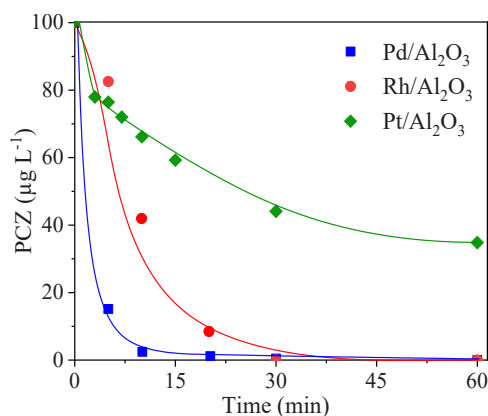


Fig. 1. Evolution of the PCZ concentration upon HDC reaction ( $[PCZ]_0 = 100 \mu\text{g L}^{-1}$ ;  $H_2 = 50 \text{ N mL min}^{-1}$ ;  $[Catalyst] = 0.25 \text{ g L}^{-1}$ ;  $25^\circ\text{C}$ ). Experimental (symbols) and trendlines (solid lines).

Table 3

Pseudo-first kinetic rate constant obtained during the HDC of PCZ at  $25^\circ\text{C}$  with the different catalysts.

	Pd/Al <sub>2</sub> O <sub>3</sub>	Rh/Al <sub>2</sub> O <sub>3</sub>	Pt/Al <sub>2</sub> O <sub>3</sub>
$k \text{ (min}^{-1}\text{)}$	0.170 ( $r^2 = 0.989$ )	0.094 ( $r^2 = 0.989$ )	0.0256 ( $r^2 = 0.989$ )

rate of PCZ. This difference in activity can be due to both the different nature of the catalyst and its lower particle size. The great influence that particle size has on the hydrodehalogenation rate has been previously reported in the literature [21].

### 3.2. Mechanism of PCZ degradation by HDC

A new set of experiments was conducted to analyze the intermediates and products formed during the HDC of PCZ using Pd/Al<sub>2</sub>O<sub>3</sub> and Rh/Al<sub>2</sub>O<sub>3</sub> catalysts, as they exhibited the highest activity in the process. To enhance the detection and identification of the different compounds formed along reaction, an initial PCZ concentration of  $10 \text{ mg L}^{-1}$  was employed, and the reaction samples collected were analysed using an HPLC-MS. As expected, the evolution of PCZ concentration during the reaction showed similar trends to those observed when operating at a PCZ concentration of  $100 \mu\text{g L}^{-1}$  (see Fig S2 and S3 of Supplementary Material for experimental data). Several reaction intermediates were obtained along the HDC of PCZ when using both Pd/Al<sub>2</sub>O<sub>3</sub> and Rh/Al<sub>2</sub>O<sub>3</sub> catalysts. In particular, two isomeric forms of a reaction intermediate containing two chlorine atoms (I-2Cl<sub>A</sub> and I-2Cl<sub>B</sub>, both with  $m/z$  values of 342.2), a reaction intermediate with a single chlorine atom (I-1Cl, with  $m/z$  value of 308.2), and a non-chlorinated compound (NCP, with  $m/z$  value of 274.2) were identified in both cases. Furthermore, in the reactions conducted with the Rh/Al<sub>2</sub>O<sub>3</sub> catalyst, the formation of a non-chlorinated compound in which the aromatic group of the original molecule was completely hydrogenated was also confirmed (HP, with  $m/z$  value of 280.2).

Figs. 2 and 3 depict the evolution of such reaction intermediates and final products during the HDC reactions conducted using Pd/Al<sub>2</sub>O<sub>3</sub> and Rh/Al<sub>2</sub>O<sub>3</sub> catalysts, respectively. Furthermore, these figures include the evolution of chloride anion concentration, which was released during the reactions.

As can be seen, the evolution of the different compounds through the reaction exhibited slight variations depending on the active catalytic phase employed. Intermediates containing one or two chlorine groups (I-1Cl and I-2Cl<sub>A</sub>, I-2Cl<sub>B</sub>) reached their maximum concentration in the initial stages of the reaction, which was shifted to shorter reaction times

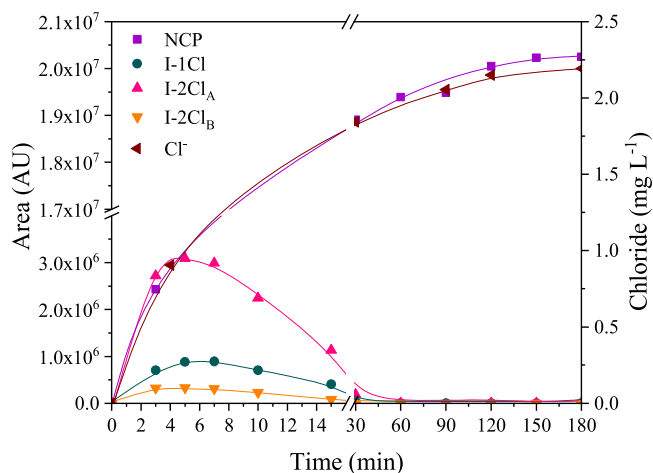
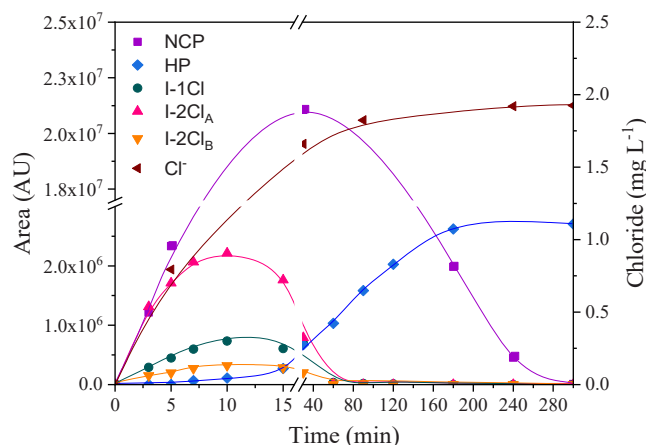


Fig. 2. Evolution of intermediates, products, and Cl<sup>-</sup> in the HDC of PCZ with the Pd/Al<sub>2</sub>O<sub>3</sub> catalyst. ( $[PCZ]_0 = 10 \text{ mg L}^{-1}$ ;  $H_2 = 50 \text{ N mL min}^{-1}$ ;  $[Pd/Al_2O_3] = 0.25 \text{ g L}^{-1}$ ;  $25^\circ\text{C}$ ).



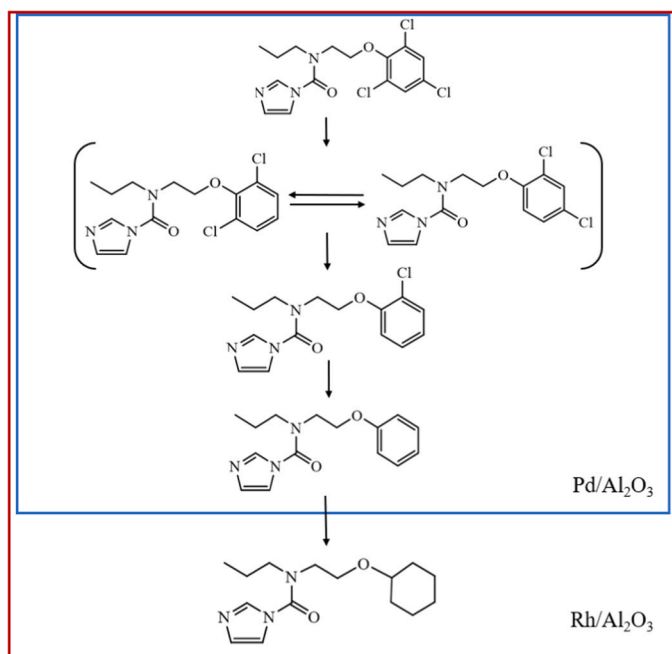


**Fig. 3.** Evolution of intermediates, products, and Cl<sup>-</sup> in the HDC of PCZ with the Rh/Al<sub>2</sub>O<sub>3</sub> catalyst. ([PCZ]<sub>0</sub> = 10 mg L<sup>-1</sup>; H<sub>2</sub> = 50 N mL min<sup>-1</sup>; [Rh/Al<sub>2</sub>O<sub>3</sub>] = 0.25 g L<sup>-1</sup>; 25 °C).

when employing the Pd/Al<sub>2</sub>O<sub>3</sub> catalyst. Nevertheless, the complete conversion of these compounds occurred before the end of the reaction regardless of the catalyst used. The compound without chlorine in its structure (NCP) was the single final product of the reaction in presence of Pd/Al<sub>2</sub>O<sub>3</sub> catalyst, whereas a maximum in its concentration was observed with the Rh/Al<sub>2</sub>O<sub>3</sub> catalyst. In the latter case, the generation of new reaction product (HP) was found. These results are in good agreement with those reported by other authors during the hydrodechlorination of different unsaturated organohalogenated compounds using Rh catalysts and can be attributed to the high hydrogenation capacity commonly associated with this active phase [37]. In any case, it should be highlighted that, regardless of the Pd/Al<sub>2</sub>O<sub>3</sub> or Rh/Al<sub>2</sub>O<sub>3</sub> considered, the final reaction products are non-halogenated compounds.

The chlorine balance calculated considering the concentration of the chlorinated products and the released HCl, exhibited a significant mismatch (23–31 %), regardless of the catalyst used. According to these results, and considering the characterization data (see Table S1 in the Supplementary Material for the carbon content of the catalysts before and after HDC reaction), a new set of adsorption experiments was subsequently carried out. The obtained results showed PCZ adsorption values of 18 % and 29 % with the Pd/Al<sub>2</sub>O<sub>3</sub> and Rh/Al<sub>2</sub>O<sub>3</sub> catalysts, respectively, which allowed closing the chlorine balances (>95 %). These results indicate that the Rh/Al<sub>2</sub>O<sub>3</sub> catalyst appears to favour pollutant adsorption to a greater extent due to the smaller particle size of the Rh particles compared to Pd/Al<sub>2</sub>O<sub>3</sub> (and Pt/Al<sub>2</sub>O<sub>3</sub>), favouring a higher number of Rh nanoparticles available for pollutant adsorption [38].

According to the identified intermediates and products, a similar reaction pathway (Scheme 1) was proposed for both catalysts (Pd/Al<sub>2</sub>O<sub>3</sub> and Rh/Al<sub>2</sub>O<sub>3</sub>) but including an additional step when the Rh/Al<sub>2</sub>O<sub>3</sub> catalyst was used. As illustrated in Scheme 1, PCZ, which contains three chlorine groups in its structure, is firstly hydrodechlorinated giving rise to two different isomers with two chlorine groups in different positions of the aromatic ring (I-2Cl<sub>A</sub> and I-2Cl<sub>B</sub>). The occurrence of these two isomers, whose commercial name is propiconazole (PPZ), has already been reported by Dalhoff et al., 2016 [39] in their study dedicated to the toxicity analysis of PCZ and PPZ. Subsequently, I-2Cl<sub>A</sub> and I-2Cl<sub>B</sub> undergo sequential hydrodechlorination stages, losing completely its chlorine content and resulting in the formation of NCP, the final reaction product for the Pd/Al<sub>2</sub>O<sub>3</sub> catalyst. As it has been abovementioned, in the case of Rh/Al<sub>2</sub>O<sub>3</sub> catalyst, an additional step took place, involving the hydrogenation of the aromatic ring to form a cyclohexyl group. It can be concluded that, whereas the Rh/Al<sub>2</sub>O<sub>3</sub> catalyst favours the hydrogenation of the double bonds, the Pd/Al<sub>2</sub>O<sub>3</sub> catalyst seems to be more active for the hydrodechlorination step [17]. Consequently, the composition of



**Scheme 1.** Reaction scheme for the HDC of PCZ with Pd/Al<sub>2</sub>O<sub>3</sub> and Rh/Al<sub>2</sub>O<sub>3</sub>.

the final effluents obtained in reaction will be influenced by the active phase of the catalyst.

### 3.3. Application of CMRs in continuous flow HDC

Several CMRs were developed using different active phases for application of HDC in continuous mode. Considering the results of the batch experiments, both Pd and Rh metals were employed, as well as a combination of them (Pd-Rh/CMR) to enhance the reaction kinetics and promote the hydrogenation stage. As representative example, Fig. 4 shows the images of the Pd/CMR at different stages of preparation (fresh material, ionic adsorption, calcination and reduction) and a STEM image of the final CMR. It must be noted that the appearance of Rh/CMR and Pd-Rh/CMR were almost the same to Pd/CMR. As can be seen, the color of the CMR surface evolved after each preparation step, going from white to reddish, black, and finally, grey material. Similar evolution was observed for the others CMRs developed in this work. Metal-based CMRs were fully characterized by different techniques and the results are summarized in Table 4.

The surface of the CMRs were coated with a thin layer of metal nanoparticles, with a size of  $5.7 \pm 1.9$  nm for Pd/CMR and  $2.6 \pm 1.1$  nm for Rh/CMR (see Fig. S4 of the Supplementary Material for STEM image of the Rh/CMR). Similar nanoparticle sizes were observed in the case of the Pd-Rh/CMR ( $5.6 \pm 1.7$  nm of Pd and  $3.8 \pm 0.8$  nm of Rh). Additionally, ICP-MS analysis confirmed the metal loading achieved on the catalysts, with values of 1.1% wt. for Pd/CMR, 0.93% wt. for Rh/CMR, and 0.45% wt. for each metal in the bimetallic CMR. The zerovalent (Me<sup>0</sup>) and electrodeficient (Me<sup>n+</sup>) molar ratios were calculated, resulting in values of 0.92, 0.97 and 1.18–1.07 for Pd/CMR, Rh/CMR and Pd-Rh/CMR, respectively (see Fig. S5-S8 of the Supplementary Material for core level spectrum of Pd 3d and Rh 3d). These results are in accordance with the optimum ratio (Me<sup>0</sup>/Me<sup>n+</sup> ~ 1) reported for the highest activity in the case of Pd catalysts during HDC reactions [21].

The activity and stability of the developed membranes in the HDC of PCZ were evaluated over a continuous 100-h operation experiment. Fig. 5 shows the PCZ concentration in the effluent during the treatment with each CMR under evaluation. In all cases, substantial PCZ removal, close to 95 %, was achieved, and the conversion remained stable throughout the entire 100-h testing period. Consequently, the developed

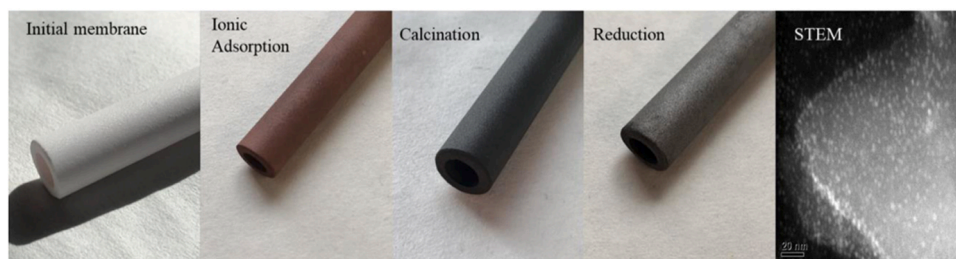


Fig. 4. Aspect of Pd/CMR during the preparation stages and STEM image of the finally obtained catalytic membrane.

**Table 4**  
Main characteristics of fresh CMRs.

Catalyst	Pd (%) wt.)	Rh (%) wt.)	Pd dp (nm)	Rh dp (nm)	Pd <sup>0</sup> / Pd <sup>a+</sup>	Rh <sup>0</sup> / Rh <sup>a+</sup>
Pd/CMR	1.01	-	5.7	-	0.92	-
Pd-Rh/ CMR	0.45	0.45	5.6	3.8	1.18	1.07
Rh/CMR	-	0.93	-	2.6	-	0.97

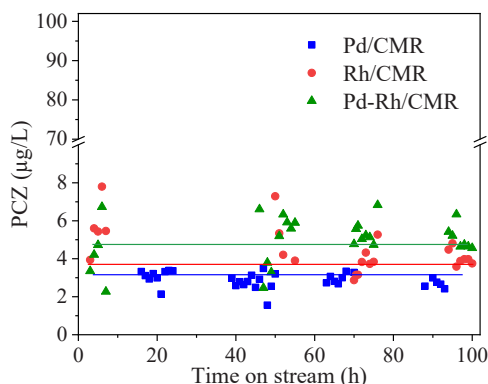


Fig. 5. Evolution of PCZ concentration in the effluent outflow during HDC reactions using different metal-supported CMRs ( $[PCZ]_0 = 100 \mu\text{g L}^{-1}$ ;  $H_2 = 50 \text{ N mL min}^{-1}$ ;  $Q_{\text{FEED}} = 1 \text{ mL min}^{-1}$ ;  $25^\circ\text{C}$ ).

CMRs exhibited both high activity and remarkable stability for the HDC reaction, regardless of the precious metal coating their surface. In contrast to the differences found in the reaction rates observed in batch operation depending on the active phase used, similar results were observed in the degradation of PCZ when CMRs were used in continuous mode. The Pd and Rh particle sizes of CMRs are close to the optimal range for hydrodehalogenation activity, which is between 4 and 8 nm, and powder catalysts except for Pd, have a lower particle size with a maximum of 3.6 nm, which may explain why they have a somewhat lower activity than CMRs [22].

Based on the obtained results with the commercial catalysts in batch mode and considering the observed independence of PCZ conversion from the initial pollutant concentration during continuous mode operation, a pseudo-first-order kinetics model was proposed to describe the HDC rate of PCZ in the CMR system [40,41]. Accordingly, from the mass balance in the reactor, the Eq. 1 was derived where  $W$  is the catalyst weight (g) (16.5 g),  $Q$  is the feed aqueous flow rate ( $\text{mL min}^{-1}$ ),  $X_{PCZ}$  is the PCZ conversion and  $k$  is the pseudo-first order rate constant which includes the  $H_2$  concentration since it is continuously supplied in considerable excess.

$$\frac{W}{F_{PCZ,0}} = \frac{W}{Q \cdot C_{PCZ,0}} = \int_0^{X_{PCZ}} \frac{dX_{PCZ}}{k \cdot C_{PCZ,0} \cdot (1 - X_{PCZ})} \quad (1)$$

For the experiments conducted using CMRs, it was considered that, in all cases, the controlling stage was the chemical reaction, with no limitation either by external or internal mass transport. This hypothesis was supported by the previous work published by Nieto-Sandoval et al. (2021) [25], where the existence of limitations due to external diffusion was ruled out during the HDC of diclofenac by a similar Pd/CMR system. The values of the pseudo-first-order apparent rate constants were 0.062, 0.06 and  $0.061 \text{ min}^{-1}$  for Pd/CMR, Rh/CMR and Pd-Rh/CMR, respectively. With regard to the product distribution (see Fig. S9 of the Supplementary Material), significant variations were observed depending on the active phase present in the CMR. In the case of Pd/CMR, the main product of the HDC reaction was NCP along with traces of the I-1Cl, I-2Cl<sub>A</sub> and I-2Cl<sub>B</sub>. In the case of Rh/CMR, again, mainly the NCP and traces of the other reaction products (I-1Cl, I-2Cl<sub>A</sub>, I-2Cl<sub>B</sub> and HP) were identified. However, when the bimetallic CMR was used, a higher proportion of I-1Cl was obtained compared to the other membranes, hindering complete dechlorination. Although these results are in good agreement with the previously proposed reaction pathways using commercial powder catalysts, it should be noted that, in contrast to the results in batch mode with the Rh/ $Al_2O_3$  catalyst, in the case of Rh/CMR, the operating conditions used in the continuous tests did not allow further hydrogenation of NCP. This can be due to the fact that further NCP hydrogenation took place once PCZ was completely removed, which was not the case under the operational conditions used for the experiments conducted in continuous mode with the CMRs. Based on these results and considering that, according to a previous study (Del Olmo et al., 2023 [16]), the effectiveness of the process in terms of toxicity reduction is directly related to the elimination of organo-halogenated species (both pollutants and chlorinated intermediates), it can be concluded that Pd and Rh-based CMRs represent a promising alternative to remove organochlorinated pollutants in aqueous streams and thus, to warrant the ecotoxicity abatement.

### 3.4. Operating conditions study

The efficiency of the HDC process for the removal of organo-chlorinated pollutants is closely tied to both the catalytic system and the operating conditions employed. Due to the high stability and activity exhibited by the Pd/CMR, as well as the high yield to non-halogenated products, this catalytic membrane was selected for conducting a comprehensive study aimed at optimizing operating conditions (aqueous flow rate, temperature and initial PCZ concentration). For each experiment, specific operating conditions were established, and the PCZ removal was followed over 24 h on stream. This methodology allowed the comparison of both the activity and stability of the system in the different experiments, using the same CMR. Fig. 6 shows a comparison of the effect of operating conditions on the value of the pseudo-first order apparent rate constant obtained. An increase in the feed flow rate, evaluated from  $0.75 \text{ mL min}^{-1}$  to  $2 \text{ mL min}^{-1}$ , led to a higher PCZ outflow concentration and, consequently, a reduction in PCZ conversion. However, similar apparent pseudo-first rate constants were obtained in all cases with values ranging from  $0.057$  to  $0.061 \text{ min}^{-1}$ . These results confirmed the absence of external diffusion limitations

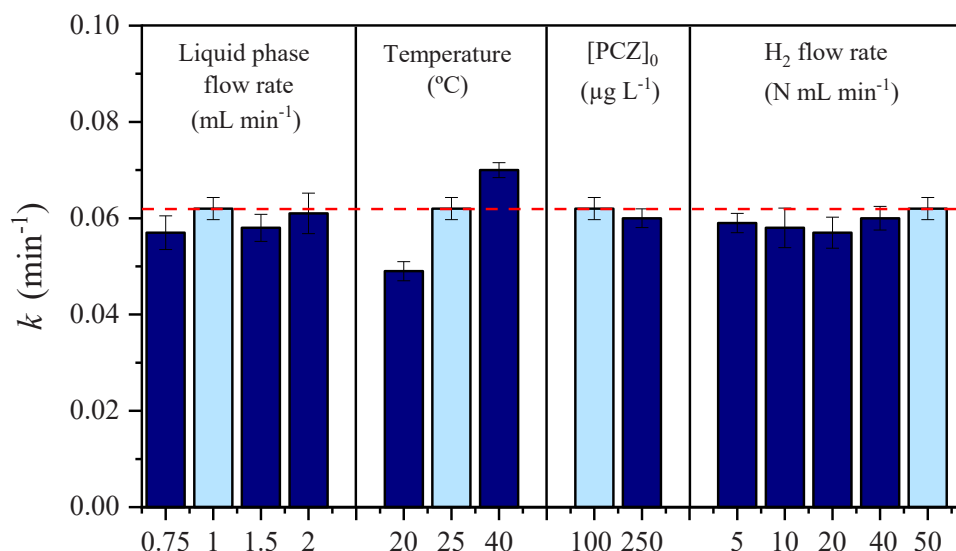


**Fig. 6.** Pseudo-first order rate constants obtained in the HDC of PCZ using Pd/CMR at different operating conditions (standard conditions:  $[PCZ]_0 = 100 \mu\text{g L}^{-1}$ ;  $H_2 = 50 \text{ N mL min}^{-1}$ ;  $Q_{\text{FEED}} = 1 \text{ mL min}^{-1}$ ;  $25^\circ\text{C}$ ).

throughout the reaction, corroborating that the process occurs under kinetic control. The pseudo-first-order rate constants obtained during the HDC of PCZ at various aqueous flow rates, were notably higher than those reported in a prior study ( $0.005 \text{ min}^{-1}$ ) where HDC of diclofenac was carried out using other Pd/CMR under similar operating conditions [25]. These differences can be attributed to both the Pd loading (1.1 wt % Pd/CMR in the current study compared to 0.2 wt% Pd/CMR in the previous one) and the chlorine content of the organochlorinated pollutant being treated (two chlorine atoms in the diclofenac molecule compared to the three chlorine atoms in the PCZ). It is widely acknowledged in the scientific literature that the dissociation energy of the carbon-halogen bond decreases with an increase in the number of halogen substituents contained in the molecule [14,42]. For instance, Mackenzie et al., (2006) [43] reported that Pd/ $\text{Al}_2\text{O}_3$  catalyst showed twelvefold higher HDC rate for the removal of tetrachloromethane compared to chloroform.

It is noteworthy that within the studied range of  $H_2$  flow rates, no significant changes were observed in the PCZ removal rate. In all cases, values of the pseudo-first-order kinetic constant close to  $0.06 \text{ min}^{-1}$  were obtained. These results demonstrate that, even with a tenfold reduction in the  $H_2$  flow rate (from 50 to 5  $\text{N mL min}^{-1}$ ), the reagent remains in sufficient excess, thereby not limiting the effectiveness of the process. Thus, the possibility of optimizing  $H_2$  consumption for the full-scale implementation of HDC becomes evident, enhancing the overall economic efficiency of the process.

The reaction temperature was also assessed within the range of 20–40°C, as shown in Fig. 6. As expected, an increase in the reaction temperature resulted in increased PCZ removal, obtaining pseudo-first kinetic constants values of 0.049, 0.062 and  $0.07 \text{ min}^{-1}$  for 20, 25 and 40 °C respectively. Applying the Arrhenius equation, an apparent activation energy of  $11.9 \text{ kJ mol}^{-1}$  and a pre-exponential factor value of  $21.2 \text{ min}^{-1}$  were obtained. According to the relatively low apparent activation energy value obtained, it can be concluded that the influence of temperature on the reaction rate in the HDC of PCZ with Pd/CMR was moderate. This observation is consistent with the findings reported in several studies in the literature where similar apparent activation energy values were obtained for the removal of several organohalogenated pollutants by HDC in the presence of Pd catalysts [44].

Finally, the response of the Pd/CMR system by varying the initial pollutant concentration fed to the reactor was assessed. The obtained results demonstrated that the initial concentration of the micropollutant

did not significantly impact PCZ conversion, consistent with a reaction described by a first-order kinetic equation. Accordingly, similar conversions values were obtained for initial PCZ concentrations of 100 and  $250 \text{ mg L}^{-1}$  (~95%), with apparent pseudo-first kinetic rate constants values of  $0.062 \text{ min}^{-1}$  and  $0.06 \text{ min}^{-1}$ , for both initial PCZ concentrations, respectively.

It is noteworthy to mention that the Pd/CMR membrane exhibited high stability throughout the HDC reaction, regardless of the operating conditions employed. All membrane properties remained practically unchanged (Table 5). Elemental analysis revealed that CMRs did not show any signs of fouling (neither by PCZ nor by the identified intermediates), as the carbon content after the HDC reaction was negligible in all cases. Unlike membranes, powdered catalysts tend to have a higher carbon content after use because they have a much larger specific surface area and thus more exposed area for the attachment of organic molecules to their structure [45]. All in all, the carbon content was quite low in all cases given the low adsorption capacity of the alumina employed as catalytic support. Furthermore, the metal content remained practically constant after the treatment, which allows ruling out possible metal leaching. In fact, TEM images of the CMRs after the long-term continuous experiment also showed metal nanoparticles homogeneously distributed on the CMR surface. In addition, the  $\text{Pd}^0/\text{Pd}^{n+}$  and  $\text{Rh}^0/\text{Rh}^{n+}$  ratios of the used CMRs were similar to those of fresh CMRs (see Fig. S10–13 of the Supplementary Material).

### 3.5. Operation in real water matrices

To demonstrate the versatility of the reaction system, tap water was tested as the reaction matrix. Analysis of the tap water revealed a total organic carbon content of  $2.5 \text{ mg L}^{-1}$ , an inorganic carbon concentration of  $2.9 \text{ mg L}^{-1}$  ( $2.3 \text{ mg L}^{-1} \text{ HCO}_3^-$  and  $0.6 \text{ mg L}^{-1} \text{ H}_2\text{CO}_3$ ), and a

**Table 5**  
Main characteristics of used CMRs.

Catalyst	Pd (% wt.)	Rh (% wt.)	Pd dp (nm)	Rh dp (nm)	$\text{Pd}^0/\text{Pd}^{n+}$	$\text{Rh}^0/\text{Rh}^{n+}$
Pd/CMR	1.03	-	5.5	-	1.01	-
Pd-Rh/CMR	0.43	0.44	5.8	3.3	0.91	0.96
Rh/CMR	-	0.9	-	3	-	1.02

chloride ion concentration of  $8.7 \text{ mg L}^{-1}$ . Additionally, sulphate and phosphate concentrations of  $7.2 \text{ mg L}^{-1}$  and  $0.2 \text{ mg L}^{-1}$  were detected, respectively. The pH value measured was 7.2 and the conductivity was  $67 \mu\text{S cm}^{-1}$ . According to the information provided by the Madrid Water Management Authority, the tap water can be classified as soft water, and clearly represents the water obtained at the final stages of a drinking water treatment plant. In this context, HDC treatment could be effectively integrated as a purification step for the removal of organochlorinated pollutants before introduction into the water supply network [46].

Fig. 7 shows the evolution of PCZ through HDC reaction in both real tap water and deionized water matrices. As can be seen, comparable results ( $\sim 95\%$  PCZ removal) were obtained under the same operating conditions with no significant changes in PCZ removal depending on the water matrix. Furthermore, it is worth noting that the product distribution obtained was highly similar regardless of the water matrix (Fig. S9 and S14 in Supplementary Material), with the non-chlorinated product being the main reaction product, exhibiting a selectivity close to 85 % in both cases. These results demonstrate the effectiveness of the system in a real water matrix. In fact, the pseudo-first order rate constant obtained in tap water is  $0.055 \text{ min}^{-1}$ , very similar to that achieved in deionised water. The slight difference observed could be due to the higher conductivity and thus the higher concentration of ions, as they can compete for the catalytic centres of Pd [43].

It is important to note that all the experiments conducted with the Pd/CMR accumulate a usage time exceeding 450 h on stream, with no deactivation observed in any case. Therefore, it can be concluded that Pd/CMR represents a highly active and remarkably stable system for the HDC process, a crucial characteristic for any potential process scale-up.

#### 4. Conclusions

HDC using Pd/ $\text{Al}_2\text{O}_3$  and Rh/ $\text{Al}_2\text{O}_3$  powder catalysts in batch-mode slurry reactors has proven to be an effective technology for the removal of organochlorinated compounds such as the target compound PCZ. In contrast, Pt/ $\text{Al}_2\text{O}_3$  catalyst exhibited signs of deactivation throughout the reaction, restricting the potential application of Pt as the active phase in HDC catalysts. Reaction pathways were proposed in accordance with the intermediates and products identified, considering the active phase of the catalysts. Complete hydrodechlorination of PCZ occurred with Pd/ $\text{Al}_2\text{O}_3$  and Rh/ $\text{Al}_2\text{O}_3$  catalysts, but an additional stage was observed when Rh catalyst was used leading to further hydrogenation of the non-chlorinated reaction product. Despite their high activity and stability, the application of these catalysts for continuous treatment of aqueous streams presents significant limitations, such as challenging catalyst recovery and high-pressure drops. In this context, CMRs constitute a feasible alternative for the subsequent scaling up of the process. Three catalytic membrane reactors with various active phases (Pd/CMR, Rh/CMR, Pd-Rh/CMR) were developed and demonstrated to exhibit both high activity and stability in the HDC of PCZ. The obtained product distribution in the treated effluent depended on the metal coating the CMR surface. NCP prevailed in Pd/CMR and Rh/CMR effluents, while Pd-Rh/CMR showed a higher proportion of I-1Cl. Optimization of Pd/CMR operating conditions revealed unaffected conversion at different initial PCZ concentrations ( $100$  and  $250 \text{ mg L}^{-1}$ ), indicative of a first-order kinetic reaction. The  $\text{H}_2$  flow rate within the assessed range ( $5\text{--}50 \text{ N mL min}^{-1}$ ) yielded no substantial alterations in the PCZ removal rate ( $k \sim 0.06 \text{ min}^{-1}$ ). This result confirmed that, under these operating conditions, hydrogen is in significant excess and does not limit the reaction rate. Varying the spatial time (feed flow rate between  $0.75$  and  $2 \text{ mL min}^{-1}$ ) while maintaining the concentration of PCZ fed to the system, allowed discarding external mass transfer limitations since similar pseudo-first order kinetic rate constant values were obtained in all cases. Temperature variation (from  $20$  to  $40^\circ\text{C}$ ) led to higher rate constant values ( $0.049$ ,  $0.062$ , and  $0.07 \text{ min}^{-1}$  at  $20$ ,  $25$ , and  $40^\circ\text{C}$ , respectively), with an activation energy close to  $11.9 \text{ kJ mol}^{-1}$ .

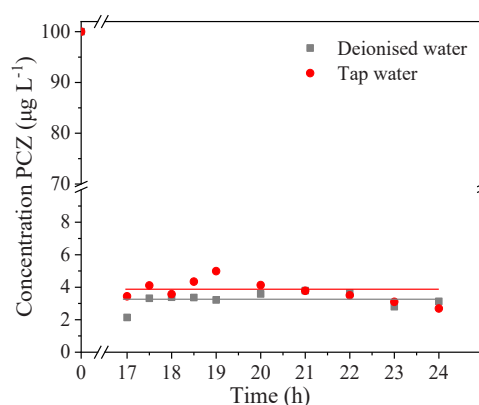


Fig. 7. Evolution of PCZ concentration in the effluent outflow during HDC reactions with Pd/CMR using tap water and deionised water ( $[\text{PCZ}]_0 = 100 \mu\text{g L}^{-1}$ ;  $\text{H}_2 = 50 \text{ N mL min}^{-1}$ ;  $Q_{\text{FEED}} = 1 \text{ mL min}^{-1}$ ;  $25^\circ\text{C}$ ).

The effectiveness of the system was finally demonstrated in a tap water obtaining similar reaction rates to those obtained using deionized water. Notably, Pd/CMR activity remained unchanged over 450 h on stream, confirming its viability for large-scale HDC applications with sustained catalytic performance. Future prospects should address the optimization of the catalytic system based on Pd/CMR for the treatment of high water flow rates with minimal hydrogen consumption.

#### CRediT authorship contribution statement

**Macarena Munoz:** Writing – original draft, Supervision, Conceptualization. **Julia Nieto-Sandoval:** Writing – review & editing. **María Torres Mendiola:** Visualization, Methodology, Investigation. **Raúl B. del Olmo:** Writing – original draft, Visualization, Methodology, Investigation. **Jose A. Casas:** Writing – review & editing, Supervision, Resources, Project administration, Funding acquisition. **Zahara M. de Pedro:** Writing – review & editing, Supervision, Conceptualization.

#### Declaration of Competing Interest

The authors declare that they have no known competing financial interests or personal relationships that could have appeared to influence the work reported in this paper.

#### Data Availability

Data will be made available on request.

#### Acknowledgments

This research has been supported by the Spanish Ministry of Science and Innovation and AEI through project PID2019-105079RB-I00 and PID2022-139063OB-I00 funded by MCIN/AEI/10.13039/501100011033 and by ERDF A way of Making Europe. J. Nieto-Sandoval and M. Munoz thanks the MINECO for the FPI contract (BES-2017-081346) and the Ramón y Cajal postdoctoral contract (RYC-2016-20648), respectively. R. B. del Olmo thanks the Operational Program for Youth Employment and the Youth Employment Initiative (YEI) of the CM for his contract as Research Assistant (PEJ-2020-AI/AMB-19161).

#### Appendix A. Supporting information

Supplementary data associated with this article can be found in the online version at [doi:10.1016/j.jece.2024.112754](https://doi.org/10.1016/j.jece.2024.112754).



## References

- [1] R.P. Schwarzenbach, T. Egli, T.B. Hofstetter, U. Von Gunten, B. Wehrli, Global water pollution and human health, *Annu. Rev. Environ. Resour.* 35 (2010) 109–136.
- [2] M. Szopińska, J. Potapowicz, K. Jankowska, A. Luczkiewicz, O. Svahn, E. Björklund, C. Nannou, D. Lambropoulou, Z. Polkowska, Pharmaceuticals and other contaminants of emerging concern in Admiralty Bay as a result of untreated wastewater discharge: Status and possible environmental consequences, *Sci. Total Environ.* 835 (2022) 155400.
- [3] C.L. Price, J.E. Parker, A.G. Warrilow, D.E. Kelly, S.L. Kelly, Azole fungicides—understanding resistance mechanisms in agricultural fungal pathogens, *Pest Manag. Sci.* 71 (2015) 1054–1058.
- [4] S. Berger, Y. El Chazli, A.F. Babu, A.T. Coste, Azole resistance in *Aspergillus fumigatus*: a consequence of antifungal use in agriculture? *Front. Microbiol.* 8 (2017) 1024.
- [5] V. Belenguer, F. Martinez-Capel, A. Masiá, Y. Picó, Patterns of presence and concentration of pesticides in fish and waters of the Júcar River (Eastern Spain), *J. Hazard. Mater.* 265 (2014) 271–279.
- [6] R. Urbatzka, A. van Cauwenberge, S. Maggioni, L. Viganò, A. Mandich, E. Benfenati, I. Lutz, W. Kloas, Androgenic and antiandrogenic activities in water and sediment samples from the river Lambro, Italy, detected by yeast androgen screen and chemical analyses, *Chemosphere* 67 (2007) 1080–1087.
- [7] N. Lopez-Arago, J. Nieto-Sandoval, M. Munoz, Z.M. de Pedro, J.A. Casas, Insights on the removal of the azole pesticides included in the EU watch list by catalytic wet peroxide oxidation, *Environ. Technol. Innov.* 29 (2023) 103004.
- [8] N. De Castro-Català, I. Muñoz, J.L. Riera, A.T. Ford, Evidence of low dose effects of the antidepressant fluoxetine and the fungicide prochloraz on the behavior of the keystone freshwater invertebrate *Gammarus pulex*, *Environ. Pollut.* 231 (2017) 406–414.
- [9] N. Elfikrie, Y. Ho, Bin, S.Z. Zaidon, H. Juahir, E.S.S. Tan, Occurrence of pesticides in surface water, pesticides removal efficiency in drinking water treatment plant and potential health risk to consumers in Tengli River Basin, Malaysia, *Sci. Total Environ.* 712 (2020) 136540.
- [10] C. Adams, Y. Wang, K. Loftin, M. Meyer, Removal of Antibiotics from Surface and Distilled Water in Conventional Water Treatment Processes, *J. Environ. Eng.* 128 (2002) 253–260.
- [11] Y. Luo, W. Guo, H.H. Ngo, L.D. Nghiem, F.I. Hai, J. Zhang, X.C. Wang, A review on the occurrence of micropollutants in the aquatic environment and their fate and removal during wastewater treatment, *Sci. Total Environ.* 29 (473) (2014) 619–641.
- [12] E. Ozturk, Applying analytical decision methods for determination of the best treatment alternative to remove emerging micropollutants from drinking water and wastewater: triclosan example, *Environ. Sci. Pollut. Res.* 25 (30) (2015) 30517–30546.
- [13] B. Han, W. Liu, J. Li, J. Wang, D. Zhao, R. Xu, Z. Lin, Catalytic hydrodechlorination of triclosan using a new class of anion-exchange-resin supported palladium catalysts, *Water Res.* 120 (2017) 199–210.
- [14] J. Zhou, Y. Han, W. Wang, Z. Xu, H. Wan, D. Yin, S. Zheng, D. Zhu, Reductive removal of chloroacetic acids by catalytic hydrodechlorination over Pd/ZrO<sub>2</sub> catalysts, *Appl. Catal. B: Environ.* 134 (2013) 222–230.
- [15] M. Munoz, M. Kasperer, B.J. Etzold, Deducing kinetic constants for the hydrodechlorination of 4-chlorophenol using high adsorption capacity catalysts, *Chem. Eng. J.* 285 (2016) 228–235.
- [16] R.B. del Olmo, J. Nieto-Sandoval, M. Munoz, Z.M. de Pedro, J.A. Casas, Application of catalytic hydrodechlorination for the fast removal of chlorinated azole pesticides in drinking water, *Sep. Purif. Technol.* 323 (2023) 124393.
- [17] J. Nieto-Sandoval, R. Sanchez, M. Munoz, Z.M. de Pedro, J.A. Casas, Catalytic hydrodehalogenation of the flame retardant tetrabromobisphenol A by alumina-supported Pd, Rh and Pt catalysts, *Chem. Eng. J. Adv.* 9 (2022) 100212.
- [18] A.N. Arias, C. Correa, A review of liquid-phase catalytic hydrodechlorination, *Ing. ía e Invest. ón* 27 (2007) 52–64.
- [19] X. Wang, J. Li, M. Fu, B. Yuan, H. Cui, Y. Wang, Fabrication and evaluation of Au–Pd core-shell nanocomposites for dechlorination of diclofenac in water, *Environ. Technol.* 36 (2015) 1510–1518.
- [20] L. Calvo, M.A. Gilarranz, J.A. Casas, A.F. Mohedano, J.J. Rodriguez, Hydrodechlorination of alachlor in water using Pd, Ni and Cu catalysts supported on activated carbon, *Appl. Catal. B: Environ.* 78 (2008) 259–266.
- [21] C.B. Molina, A.H. Pizarro, J.A. Casas, J.J. Rodriguez, Aqueous-phase hydrodechlorination of chlorophenols with pillared clays-supported Pt, Pd and Rh catalysts, *Appl. Catal. B: Environ.* 148–149 (2014) 330–338.
- [22] E. Diaz, A.F. Mohedano, J.A. Casas, L. Calvo, M.A. Gilarranz, J.J. Rodriguez, Comparison of activated carbon-supported Pd and Rh catalysts for aqueous-phase hydrodechlorination, *Appl. Catal. B: Environ.* 106 (2011) 469–475.
- [23] A. Koekemoer, A. Luckos, Effect of material type and particle size distribution on pressure drop in packed beds of large particles: Extending the Ergun equation, *Fuel* 158 (2015) 232–238.
- [24] J. Lefevre, M. Gysen, S. Mullens, V. Meynen, J. Van Noyen, The benefit of design of support architectures for zeolite coated structured catalysts for methanol-to-olefin conversion, *Catal. Today* 216 (2013) 18–23.
- [25] A. Müller, M. Ludwig, M. Arlt, R. Lange, Evaluation of reactor concepts for the continuous production of fine chemicals using the selective hydrogenation of cinnamaldehyde over palladium catalysts, *Catal. Today* 241 (2015) 214–220.
- [26] J. Wegner, S. Ceylan, A. Kirschning, Ten key issues in modern flow chemistry, *Chem. Commun.* 47 (2011) 4583–4592.
- [27] O. Osegueda, A. Dafinov, J. Llorca, F. Medina, J. Sueiras, In situ generation of hydrogen peroxide in catalytic membrane reactors, *Catal. Today* (2012) 128–136.
- [28] J. Nieto-Sandoval, E. Gomez-Herrero, M. Munoz, Z.M. de Pedro, J.A. Casas, Palladium-based catalytic membrane reactor for the continuous flow hydrodechlorination of chlorinated micropollutants, *Appl. Catal. B: Environ.* 293 (2021) 120235.
- [29] O. Osegueda, A. Dafinov, J. Llorca, F. Medina, J. Sueiras, Heterogeneous catalytic oxidation of phenol by in situ generated hydrogen peroxide applying novel catalytic membrane reactors, *Chem. Eng. J.* 262 (2015) 344–355.
- [30] V.C. Sarasidis, K.V. Plakas, S.I. Patsios, A.J. Karabelas, Investigation of diclofenac degradation in a continuous photo-catalytic membrane reactor. Influence of operating parameters, *Chem. Eng. J.* 239 (2014) 299–311.
- [31] Y. Luo, C. Zhou, Y. Bi, X. Long, B. Wang, Y. Tang, et al., Long-term continuous co-reduction of 1,1,1-trichloroethane and trichloroethene over palladium nanoparticles spontaneously deposited on H<sub>2</sub>-transfer membranes, *Environ. Sci. Technol.* 55 (2020).
- [32] J. Howiezi, S. Taghvaei-Ganjali, M. Malekzadeh, F. Motiee, S. Sahebdelfar, Effect of the distribution and dispersion of palladium nanoparticles on the reducibility and performance of Pd/Al<sub>2</sub>O<sub>3</sub> catalyst in liquid-phase hydrogenation of olefins, *Reaction Kinetics, Mech. Catal.* 130 (2020) 777–795.
- [33] P. Munnik, P.E. de Jongh, K.P. de Jong, Recent Developments in the Synthesis of Supported Catalysts, *Chem. Rev.* 115 (2015) 6687–6718.
- [34] J. Nieto-Sandoval, M. Munoz, Z.M. de Pedro, J.A. Casas, Catalytic hydrodechlorination as polishing step in drinking water treatment for the removal of chlorinated micropollutants, *Sep. Purif. Technol.* 227 (2019) 115717.
- [35] M. Munoz, Z.M. de Pedro, J.A. Casas, J.J. Rodriguez, Improved γ-alumina-supported Pd and Rh catalysts for hydrodechlorination of chlorophenols, *Appl. Catal. A: Gen.* 488 (2014) 78–85.
- [36] P. Dini, J.C.J. Bart, N. Giordano, Properties of polyamide-based catalysts. Part I. Hydrodehalogenation of chlorobenzene, *J. Chem. Soc., Perkin Trans. 2* (1975) 1479–1482.
- [37] C.B. Molina, A.H. Pizarro, J.A. Casas, J.J. Rodriguez, Enhanced Pd pillared clays by Rh inclusion for the catalytic hydrodechlorination of chlorophenols in water, *Water Sci. Technol.* 65 (2012) 653–660.
- [38] M.J. Ndolomingo, R. Meijboom, Kinetics of the catalytic oxidation of morin on γ-Al<sub>2</sub>O<sub>3</sub> supported gold nanoparticles and determination of gold nanoparticles surface area and sizes by quantitative ligand adsorption, *Appl. Catal. B: Environ.* 199 (2016) 142–154.
- [39] K. Dalhoff, M. Gottardi, A. Kretschmann, N. Cedergreen, What causes the difference in synergistic potentials of propiconazole and prochloraz toward pyrethroids in *Daphnia magna*? *Aquat. Toxicol.* 172 (2016) 95–102.
- [40] M.R. Flid, L.M. Kartashov, Y.A. Treger, Theoretical and applied aspects of hydrodechlorination processes: catalysts and technologies, *Catalysts* 10.2 (2020) 216.
- [41] S. Ordóñez, B.P. Vivas, F.V. Díez, Minimization of the deactivation of palladium catalysts in the hydrodechlorination of trichloroethylene in wastewaters, *Appl. Catal. B: Environ.* 95 (3–4) (2010) 288–296.
- [42] R. Muftikian, Q. Fernando, N. Korte, A method for the rapid dechlorination of low molecular weight chlorinated hydrocarbons in water, *Water Res.* 29. 10 (1995) 2434–2439.
- [43] K. Mackenzie, H. Frenzel, F.D. Kopinke, Hydrodehalogenation of halogenated hydrocarbons in water with Pd catalysts: Reaction rates and surface competition, *Appl. Catal. B: Environ.* 63 (2006) 161–167.
- [44] Y. Li, E. Boone, M.A. El-Sayed, Size effects of PVP–Pd nanoparticles on the catalytic Suzuki reactions in aqueous solution, *Langmuir* 18 (12) (2002) 4921–4925.
- [45] J. Nieto-Sandoval, M. Munoz, Z.M. de Pedro, J.A. Casas, Application of catalytic hydrodehalogenation in drinking water treatment for organohalogenated micropollutants removal: a review, *J. Hazard. Mater. Adv.* 5 (2022) 100047.
- [46] G. Yuan, M.A. Keane, Role of base addition in the liquid-phase of 2, 4-dichlorophenol over Pd/Al<sub>2</sub>O<sub>3</sub> and Pd/C, *J. Catal.* 225 (2004) 510–522.